Colloids and Surfaces A: Physicochem. Eng. Aspects 465 (2015) 39–46

Contents lists available at ScienceDirect

Colloids and Surfaces A: Physicochemical and Engineering Aspects

journal homepage: www.elsevier.com/locate/colsurfa

Review

Cation-induced self-assembly of an amphiphilic perylene diimide derivative in solution and Langmuir–Blodgett films

Lei Zou[a], Ao You[a], Jingang Song[a], Xingzhen Li[a], Marcel Bouvet[b], Weiping Sui[a], Yanli Chen[a,*]

[a] Shandong Provincial Key Laboratory of Fluorine Chemistry and Chemical Materials, School of Chemistry and Chemical Engineering, University of Jinan, Jinan 250022, China
[b] Institut de Chimie Moléculaire de l'Université de Bourgogne, CNRS UMR 5260, Université de Bourgogne, 21078 Dijon, France

HIGHLIGHTS

- A new amphiphilic, unsymmetrical 15C5PDI compound was synthesized.
- Cation-induced aggregation from J-type into H-type was obtained.
- Fluorescence emission change from "switch-on" to "switch-off" is observed.
- Nanostructures formed at various air/liquid interface with different morphology.
- A significantly enhanced conductivity was obtained from 1D nanofibrils of 15C5PDI.

GRAPHICAL ABSTRACT

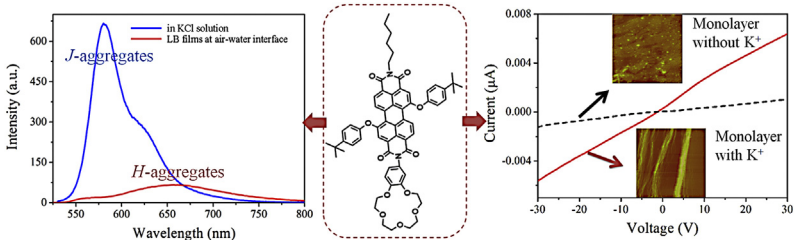

ARTICLE INFO

Article history:
Received 15 July 2014
Received in revised form
30 September 2014
Accepted 6 October 2014
Available online 16 October 2014

Keywords:
Perylenetetracarboxylic diimide
Cation-induced self-assembly
LB films
J-aggregates
H-aggregates
Conductivity

ABSTRACT

A novel amphiphilic perylenetetracarboxylic diimide (PDI) derivative, N-(4′-benzo-15-crown-5-ether)-N-hexyl-1,7-di(4-tert-butyl-phenoxy)perylen-3,4,9,10-tetracarboxylic diimide (15C5PDI), has been synthesized and characterized. Dimerization of 15C5PDI is induced in $CHCl_3$ solution with the present of K^+, resulting in the formation of the slipped co-facial *J*-aggregates, as revealed by absorption and fluorescence spectroscopies. Analysis of the surface pressure–area (π–*A*) isotherms and spectral change for the monolayer formed at the air/water interface, disclosed that 15C5PDI molecules adopted the *H*-type aggregation mode with a face-to-face configuration and edge-on orientation on both the surface of pure water and K^+ aqueous solution. Consequently, a particularly interesting fluorescence emission change from "switch-on" to "switch-off" could be observed upon aggregation that was accompanied by a transformation from strongly fluorescent *J*-type into non-fluorescent *H*-type packing of the 15C5PDI dyes. Depending mainly on the coordination bonding between 15-crown-5-ether groups and K^+ ions, one dimensional nanofibrils formed on the surface of the K^+ aqueous solution with a more closely arrangement of 15C5PDI molecules relative to those on pure water subphase revealed by the π–*A* isotherms and atomic force microscopy (AFM) images. X-ray diffraction studies indicate that the film crystallinity and general molecular order in the Langmuir–Blodgett (LB) films deposited from the KCl solution are improved effectively in comparison with those from pure water subphase. Furthermore, the conductivity of the LB films prepared in K^+ solution is more than ca. 1 order of magnitude higher than those from water.

* Corresponding author. Tel.: +86 0531 89736150.
E-mail address: chm_chenyl@ujn.edu.cn (Y. Chen).

http://dx.doi.org/10.1016/j.colsurfa.2014.10.021
0927-7757/

Contents

1. Introduction

The construction of nano-structures with controlled morphology for π-conjugated organic molecules and programming supramolecular interaction have received increasing research interests due to the technical requirements for the development of efficient electronic and optoelectronic devices [1–3]. The major driving force operating in these precisely controlled nanoscopic architectures arises from various non-covalent interactions including π–π interaction, van der Waals forces, hydrogen bonding, hydrophilic/hydrophobic interactions, electrostatic and metal–ligand coordination. As a result, comprehensive understanding the interplay among these factors in both solution and the thin solid films to finely tune the packing model of organic molecules has formed the focus of current research interests in this field [4–6]. As an important functional dye with outstanding photo and chemical stability as well as interesting photophysical and photochemical properties, perylenetetracarboxylic diimide derivatives (PDIs) have been intensively studied as advanced molecular materials for sensors [7], organic solar cell [8] and organic field-effect transistors (OFETs) applications [9–11]. Considerable efforts have been devoted to correlating the relationship between the π-orbital overlap among neighboring conjugated molecules and carrier transport properties aiming for improving their performance [12–16]. For instance, substituents were incorporated to pentacene molecules to prevent C—H···π forces and induce more effective π–π interactions between pentacence molecules, thus leading to improved OFET properties [17–20]. Very recently, we have designed and prepared a cyclophane of perylene tetracarboxylic diimide (PDI) with four phenoxy substituents at the bay positions of the two PDI rings, which were revealed to show unexpectedly good n-type OFET properties and device environmental stability resulting from the formation of intra- and inter-molecular *H*-aggregates associated with the segregation effects imparted by the flexible hydrophobic alkyl substituents at the imide nitrogens of the PDI molecule [21,22]. It is worth noting that a significant effort has been made toward self-assembly of symmetrical PDI derivatives into one-dimentional (1D) nanostructures including nanobelts [23,24], nanotubes [25,26] and nanofibers [27,10]. Depending mainly on intermolecular π–π stacking, the 1D alignment of π-conjugated molecules facilitates carrier transport, which enables their applications in optoelectronic devices. We have also designed and prepared a series of symmetrical PDI derivatives, and found that the nanostructural morphology was affected by both molecular modification and the solvent effect [28,29,9,30–32]. Langmuir and Langmuir–Blodgett (LB) techniques are useful tools to fabricate monolayer and/or multilayer films with controllable structure and molecular orientations in the molecular level [33]. However, the application of LB techniques in the construction of nanostructure for unsymmetrical PDI derivative having the different hydrophobic/hydrophilic substituents is scarcely reported so far probably because of the difficulties on the synthesis of unsymmetrical, amphiphilic PDIs [34]. For the purpose of extensive studies, we describe herein the synthesis and characteristics of a new unsymmetrical, amphiphilic perylenetetracarboxylic diimide (PDI) derivative with a hydrophilic 4-benzo-15-crown-5-ether unit and a hydrophobic alkyl chain linked at the imide nitrogen positions, named as N-(4′-benzo-15-crown-5-ether)-N-hexyl-1,7-di(4-tert-butyl-phenoxy)perylen-3,4,9,10-tetracarboxylic diimide (15C5PDI), Scheme 1. The introduction of functional crown ether group having remarkable recognition and metal binding ability at the one side of imide nitrogen position on the PDI ring make it possible to tune molecular packing mode by cation-induced self-assembly, while hydrophobic linear alkyl chain linked at the another side of imide nitrogen position is to expected to provide sufficient flexibility for the optimization of the noncovalent stacking of the perylene diimide π systems. We show that this amphiphilic molecule self-assembled into a dimeric double-decker structure in solution and 1D nanofibrils formed from complementary coordination between crown ether and alkali ions at an air/water interface. In addition, the significantly improved semiconducting properties of the nanostructures fabricated from 15C5PDI in the presence of potassium ions relative to these in the absence of potassium ions, are also revealed by *I–V* measurements.

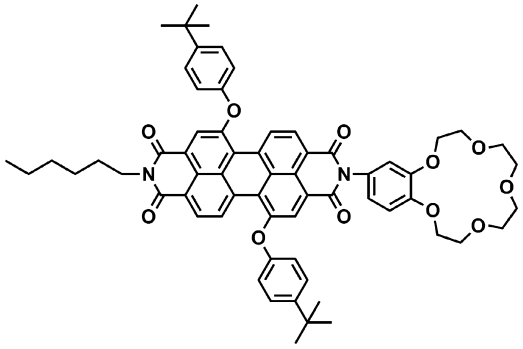

Scheme 1. The molecular structure of 15C5PDI.

2. Experimental

2.1. Chemicals

4-Aminobenzo-15-crown-5-ether was purchased from Tokyo Chemical Industry Co., Ltd. All other reagents and solvents were

used as received. Column chromatography was carried out on silica gel. All other chemicals and solvents were reagent grade and used as received without further purification.

2.2. General method

Electronic absorption spectra were recorded on a Hitachi U-4100 spectrophotometer. Fluorescence spectra were measured on a FLS920 at room temperature. The fluorescence quantum yields were calculated with N,N-dicyclohexyl-1,7-di(4-tert-butyl)phenoxyperylene-3,4,9,10-tetracarboxylate diimide as standard. AFM images were collected in air under ambient conditions using the tapping mode with a NanoscopeIII/Bioscope scanning probe microscope from Digital instruments. X-ray diffraction experiment was carried out on a Bruker AXS D8 ADVANCE X-ray diffractometer. LB films were prepared in an alternate layer Langmuir–Blodgett trough equipped with a Wilhelmy plate to measure the surface pressure.

2.3. Synthesis of N-(4′-benzo-15-crown-5-ether)-N-hexyl-1,7-di(4-tert-butyl-phenoxy) -perylen-3,4,9,10-tetracarboxylic diimide (15C5PDI)

The detailed synthetic procedures of the unsymmetrically substituted amphiphilic PDI derivative, 15C5PDI, together with the structure characterization are described in Supplementary material (Scheme S1).

2.4. Electrical experiments

The fundamental electrical measurements of 15C5PDI LB films fabricated from water surface and 0.005 mol L^{-1} potassium chloride surface were performed using a Hewlett-Packard (HP) 4140B parameter analyzer at room temperature. Current–voltage (*I–V*) curves were registered in the −30 to 30 V voltage range with 1 V increments. The interdigitated electrode (IDE) array is composed of 10 pairs of ITO electrode digits deposited onto a glass substrate with the following dimensions: 125-μm electrode width, 75-μm spacing, 5850-μm overlapping length, and 20-nm electrode thickness. The conductivity can be calculated according to the equation reported in the previous literatures [35,36].

3. Results and discussion

3.1. UV–vis absorption and fluorescence spectra in solution

The electronic absorption and emission spectra of 15C5PDI in $CHCl_3$ (10^{-5} mol L^{-1}) and in the presence of K^+ ions (5×10^{-6} mol L^{-1}) with the concentration ratio of $[K^+]/[15C5PDI] = 0.5$ in this solution are characteristic (Fig. 1). For 15C5PDI in $CHCl_3$, the absorptions at about 549 and 514 nm can be attributed to the 0–0 and 0–1 vibronic band of the S_0–S_1 transition, respectively, while the observed absorption band around 407 nm to the electronic S_0–S_2 transition, Fig. 1 (solid line). The good agreement of the peak positions and extinction coefficients for 15C5PDI with those observed for similar PDI derivatives bearing other substituents on the imide nitrogen is explained by the presence of nodes in the HOMO and LUMO at this position [28,37–40]. The fluorescence spectrum of 15C5PDI in $CHCl_3$ presented as a mirror image of the S_0–S_1 absorption band with an emission maximum at ca. 574 nm, Fig. 1 (solid line). The peak positions and vibronic fine structure correspond well to those of known PDIs with a similar substitution pattern at the bay positions [32,41,42]. After potassium ions were added into the solution of 15C5PDI with a concentration ratio of $[K^+]/[15C5PDI] = 0.5$ in this solution, the absorption of 15C5PDI

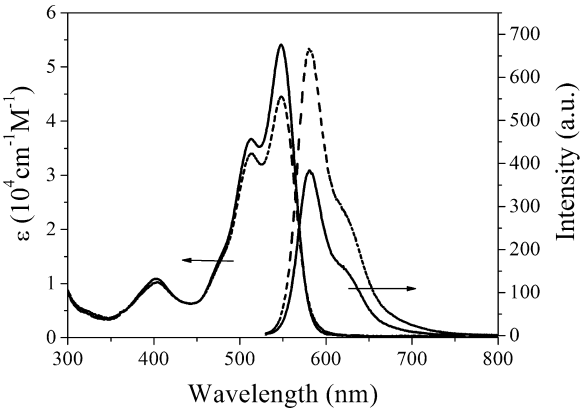

Fig. 1. UV–vis absorption (left) and fluorescence spectra (right) of 1×10^{-5} mol L^{-1} 15C5PDI in chloroform solution (solid line) and after addition of K^+ ions (KCl) with the concentration ratio of $[K^+]/[15C5PDI] = 0.5$ in this solution (dash line). The excited wavelength was 515 nm.

changed significantly in the ratio of the intensities of the 0–0/0–1 peaks, while peak positions of absorption maxima of 15C5PDI remained almost unaltered, Fig. 1 (dashed line). This phenomenon was an indication of parallel center-to-center transition dipole moments of two perylene moieties in the *J*-type aggregates in which 15C5PDI molecules form a slipped co-facial configured species by complexation of the crown ether units of 15C5PDI molecules with potassium ions [43,44]. Most interestingly, the fluorescence of the aggregated state was increased in comparison with that of the monomeric state, while the emission maximum remained essentially the same, but with the loss of fine structure Fig. 1 (dashed line). Additionally, fluorescence spectra of 15C5PDI with various mole rations of K^+ ions have been measured by the quantitative titration experiments of 15C5PDI (10^{-5} mol L^{-1}), Fig. S1 (Supplementary material). We observed a gradually increase in the emission intensity by gradual addition of K^+ ions into solution of 10^{-5} mol L^{-1} 15C5PDI (from $[K^+]/[15C5PDI] = 0$ to 1 with a step of 0.1), which more clearly confirm the effect of ionic strength and aggregation on fluorescence spectra in solution. Concomitantly, the fluorescence quantum yield of 15C5PDI is improved from 5.2% for the isolated 15C5PDI to about 13.6% upon aggregation. As a consequence, the "switch-on" of the fluorescence of 15C5PDI is achived during the transition from the monomeric state into the aggregated state upon addition of K^+ ions which fits well with the feature of *J*-type packing of the PDI dyes [41]. Furthermore, fluorescence decay time of the 15C5PDI solution without and with K^+ ions was also measured respectively, Fig. S2 (Supplementary material). A single component exponential population decay with a time constant of 0.1766 ns was obtained for 15C5PDI solution alone, while a two component exponential population decay for 15C5PDI solution with K^+ was revealed with time constants of 0.1816 ns (20.4%) and 4.3267 ns (79.6%). According to earlier researches for PDI-based donor-accepter fluorophores [25,45–47], the shorter lifetimes obtained for 15C5PDI solution alone or in the presence of K^+ are likely due to a photoinduced electron transfer from covalently linked 15-crown-5 macrocyclic unit (as donor) to PDI core (as accepter) within 15C5PDI, while the component of 4.3267 ns can be assigned to the fluorescence of PDI core. As K^+ ions were added into 15C5PDI solution, the intramolecular electron transfer within 15C5PDI was inhibited, and as a result the fluorescence of PDI core was restored due to the interaction between 15-crown-5 macrocyclic units and K^+ ions.

The detailed process of K^+-induced self-assembly of the 15C5PDI was examined by K^+-triggered spectroscopic evolution of 15C5PDI in the region of 350–650 nm recorded in $CHCl_3$, as shown in Fig. 2. Compared with two main absorption bands at 549 nm and 514 nm

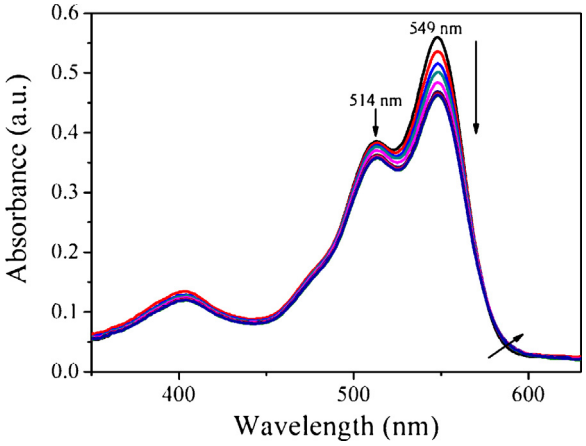

Fig. 2. Absorption spectra of 15C5PDI with various mole rations of K^+ ions. KCl (10^{-3} mol L^{-1}) in $CHCl_3/CH_3OH$ (95:5, v/v) was added gradually to a solution of 15C5PDI (10^{-5} mol L^{-1}, 3 mL) in $CHCl_3$. The arrows indicate the direction of the spectroscopic change from progressively increasing the concentration ratio of K^+ ions to 15C5PDI: $[K^+]/[15C5PDI]$ from 0 to 1 with a step of 0.1(the concentration of K^+ from 0 to 10^{-5} mol L^{-1} with a step of 10^{-6} mol L^{-1}).

in chloroform as free monomer, the decrease for low-energy 0–0 transition absorption at 549 nm was more obvious than the high-energy 0–1 band at 514 nm with gradual addition of K^+ ions into solution of 10^{-5} mol L^{-1} 15C5PDI (from $[K^+]/[15C5PDI] = 0$ to 1 with a step of 0.1, and the concentration of K^+ from 0 to 10^{-5} mol L^{-1} with a step of 10^{-6} mol L^{-1}). As a result, the relative intensity of 0–1 transition absorption increased, suggesting strong π–π stacking and a typical *J*-type aggregation behavior with slipped co-facial dimer formation [32,42,48]. Furthermore, the dimer formation was monitored by variation of the absorbance at 514 nm (the so-called dimer band) and 549 nm (monomer band) of 15C5PDI during addition of KCl in $CHCl_3/CH_3OH$ (95:5, v/v). As can be seen from Fig. 3, the change almost saturates until $[K^+]/[15C5PDI]$ value reach about 0.5, in particular the change of the monomer peak is most sharp in the region of $0 < [K^+]/[15C5PDI] \leq 0.5$, indicating that encapsulation probably continues until the available sites are saturated, i.e. until two 15-crown-5 macrocyclic units from two 15C5PDI molecules bind one K^+ ion in a eclipsed dimer.

$$nK^+ + 2\,\text{monomer(15C5PDI)} \overset{K}{\rightleftharpoons} \text{dimer} \cdot K_n^+ \text{(15C5PDI} - K_n^+ - \text{15C5PDI)} \quad (1)$$

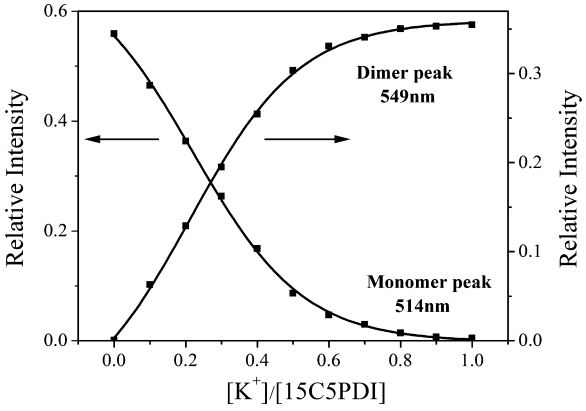

Fig. 3. Variation of the absorbance at 514 and 549 nm of 15C5PDI during addition of KCl in $CHCl_3/CH_3OH$ (95:5, v/v). The curve going up with $[K^+]$ represents the change at dimer peak and should be referred to the right axis, while that going down is the change at monomer peak and should be referred to the left axis.

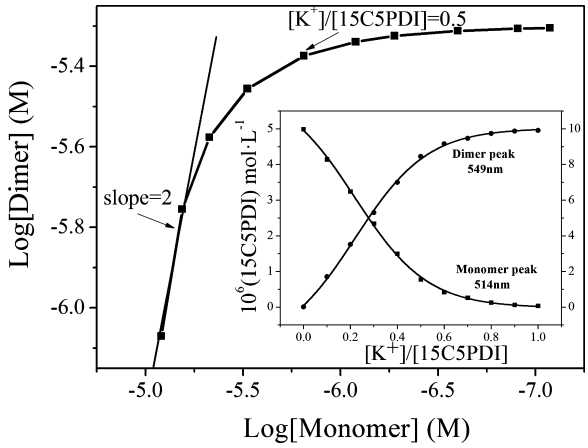

Fig. 4. Plot of log [Monomer] vs. log [Dimer·K^+] in $CHCl_3/CH_3OH$. The inset shows the dependence of monomer and dimer concentrations on $[K^+]/[15C5PDI]$.

Eq. (1) is proposed with the speculation that the equilibrium between monomer 15C5PDI (upon addition of K^+ ions) and the corresponding dimer, (15C5PDI–K^+–15C5PDI) should be exist in the present system. The monomer and dimer concentrations could be calculated from the spectral changes during titration using the method described by West and Pearce [49]. If Eq. (1) was available, the slope of 2 from a plot of log [monomer] vs. log [dimer·K^+] would be obtained. As expected, a region with slope ≈2.0 continues until $[K^+]/[15C5PDI]$ = ca. 0.5 (Fig. 4). Consequently, the complete conversion from monomer to dimer with a very high formation constant, $K = (8.1 \pm 0.2) \times 10^{11}$ L^2 mol^{-2}, for Eq. (1) with $n = 1$ is obtained, when two 15C5PDI units bind one cation. After this point ($[K^+]/[15C5PDI] = 0.5$), the slope of the plot approaches zero, especially beyond the region $[K^+]/[15C5PDI] > 1$, revealing that dimerization is not occurring in this region, Fig. 4.

3.2. *The solid state packing and optical properties of 15C5PDI in Langmuir–Blodgett (LB) films*

To further insight into the effect of packing mode on optical properties, we prepared a completely aggregated film of amphiphilic 15C5PDI by Langmuir–Blodgett method [50]. Based on the pressure–area (π–*A*) isotherms for the monolayer of 15C5PDI on the surfaces of pure water and 0.005 mol L^{-1} KCl aqueous solution at room temperature, the limiting molecular areas (extrapolated to $\pi = 0$ for condensed region) of 1.24 and 1.06 nm^2 per molecule were obtained, respectively (Fig. 5A). These values are considered to correspond to the mean molecular area of the slipped cofacial 15C5PDI molecules stacked closely with an "edge-on" configuration in the monolayers, where the long axis of 15C5PDI molecules is almost perpendicular to the surface of both pure water and KCl aqueous solution (Fig. 5B and C), in comparison with the corresponding energy-optimized conformation obtained from DFT calculation (Supplementary material, Scheme S2). Therefore, the conjugated π planes face each other to form π-stacked aggregates. Furthermore, a smaller molecular area (1.06 nm^2 per molecule) of 15C5PDI on the KCl subphase relative to that on the pure water subphase (1.24 nm^2 per molecule) implied the formation of a more compact structure due mainly to the binding effect of K^+ ions between adjacent 15C5PDI molecules associated with the strong hydrophobic interaction among the long alkyl chains of adjacent 15C5PDI molecules in addition to the π–π stacking interaction between the PDI rings. It is worth noting that the π–*A* isotherms of the 15C5PDI change depending on the KCl concentration in the subphase (Supplementary material, Fig. S3), while the corresponding experimental data are compiled in Table S1 (Supplementary material).

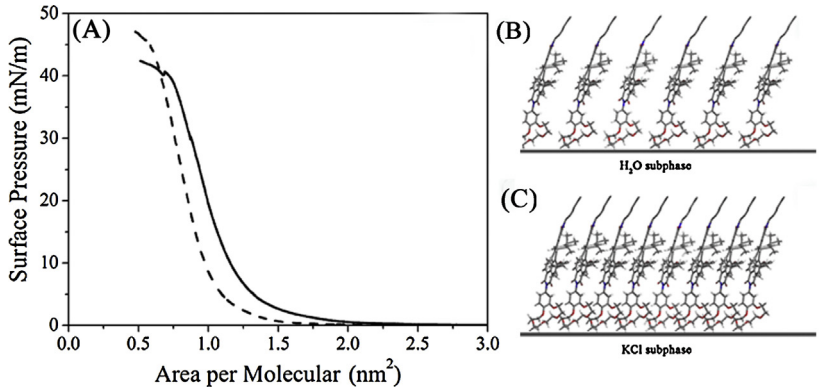

Fig. 5. π–*A* isotherms of 15C5PDI (A) on the surface of water (solid line) and 0.005 mol L^{-1} KCl aqueous solution (dash line); schematic arrangement of 15C5PDI on the surface of water (B) and 0.005 mol L^{-1} KCl aqueous solution (C).

The absorption and fluorescence spectra of LB films of 15C5PDI deposited on quartz from the surface of water are essentially the same as those from KCl solution in which aggregation is induced by K^+ ions (Fig. 6, lines a and b), implying the similar packing model for 15C5PDI molecules in the LB films with or without KCl. The obvious band broadening was observed for both absorption and fluorescence in the LB films relative to that in solutions (Fig. 6, lines c and d), which could be ascribed to the effect of the closely compacted molecular assembly. In comparison with the absorption spectra of 15C5PDI in solutions, the absorption spectra of both

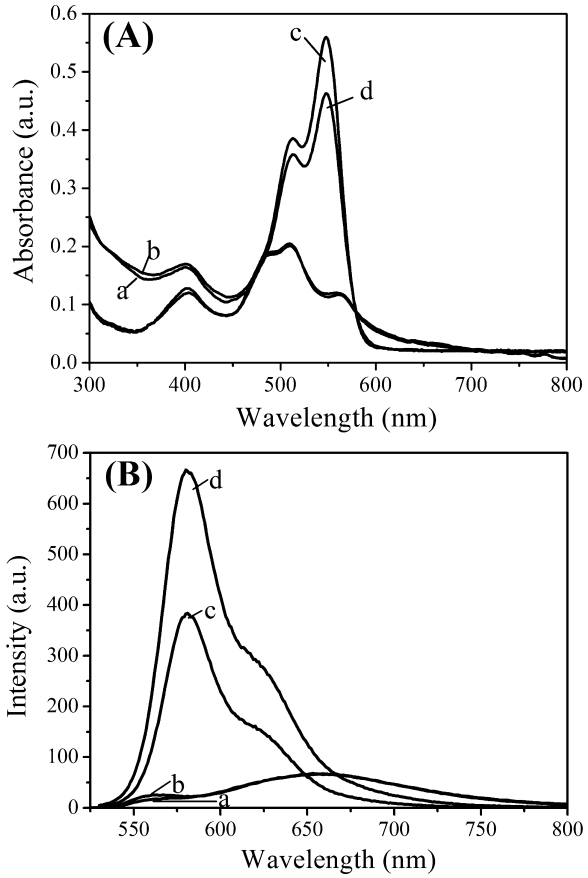

Fig. 6. UV–vis absorption (A) and fluorescence spectra (B) of 15C5PDI LB films deposited from water (line a) and 0.005 mol L^{-1} aqueous KCl surface (line b); 1×10^{-5} mol L^{-1} 15C5PDI in $CHCl_3$ solution (line c) and after addition of K^+ ions with $[K^+]/[15C5PDI] = 0.5$ (the concentration of K^+ was 5×10^{-6} mol L^{-1}) in this solution (line d). The excited wavelength was 515 nm.

LB films show a blue-shifted component with a broad maximum at 510 nm (0–1 band) and an red-shifted component at 560 nm (0–0 band), meanwhile the intensity of the vibrational transitions within the progression follows the order 0–1 > 0–0 (Fig. 6A). This indicates that for 15C5PDI there is a greater π-electron delocalization in the LB films than in solutions caused by the more planar conformation of the PDI macrocycle and closely packed face-to-face π stacks in *H*-type aggregates. Consistent with the absorption measurement, the emission spectra of the 15C5PDI LB films showed a significant red shift (about 78 nm) of the emission maxima with the loss of fine structure and significant broadening upon aggregation (Fig. 6B). The emission maxima in the longer wavelength region as compared to that in solutions should be attributed to emission from the low-energy exciton state of *H*-aggregates formed by the interaction between adjacent 15C5PDI molecules in a cofacial arrangement [30,42,51]. Particularly, in contrast to the significantly enhanced fluorescence for aggregates of 15C5PDI in KCl solution, the drastically quenched fluorescence in LB films could be observed in comparison with aggregated 15C5PDI in KCl solution. The fluorescence quenching efficiency is calculated to be as high as 90%. This further confirmed the different stacking of 15C5PDI molecules in their aggregates accompanied by a transformation from strongly fluorescent *J*-type into non-fluorescent *H*-type packing of the molecules [41].

3.3. Structural characterization of the 15C5PDI LB films

The quality of deposited LB films of 15C5PDI has been further assessed using X-ray diffraction (XRD) technique. The LB films of 15C5PDI deposited from the surface of water or potassium chloride solution give clear diffraction peaks in their low angle region, Fig. 7. The XRD diagram of the LB films deposited from the surface of water (Fig. 7A), shows a broad (0 0 1) Bragg diffraction peak falling at $2\theta = 3.64^\circ$, corresponding to an interlayer spacing of 2.43 nm according to the Bragg equation. That *d*-spacing is assigned to the distance between two adjacent 15C5PDI molecules in the longitudinal direction. Comparison between above-mentioned low-angle XRD result (2.43 nm) and a geometry-optimized, molecular length of 15C5PDI (2.60 nm, Supplementary material, Scheme S2), leads to such a conclusion that the molecules are packing with the molecular plane titled to the substrate surface in which the tilt angles of the PDI rings are around 69.2°. This implied the formation of *H*-type (face-to-face) aggregation based on the exciton theory [38]. As shown in Fig. 7B, in the low-angle range, the XRD diagram of LB films of 15C5PDI deposited from the surface of ion-containing subphase shows two well-defined diffraction peaks at $2\theta = 3.64^\circ$ and 11.8°, which are ascribed to the diffractions from the (0 0 1) and (0 0 3) planes, respectively. This implies that LB films

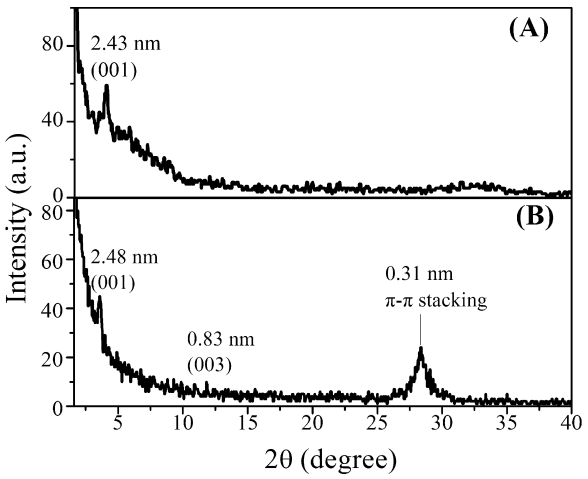

Fig. 7. X-ray diffraction patterns of 15C5PDI LB films formed on water surface (A) and 0.005 mol L^{-1} potassium chloride surface (B).

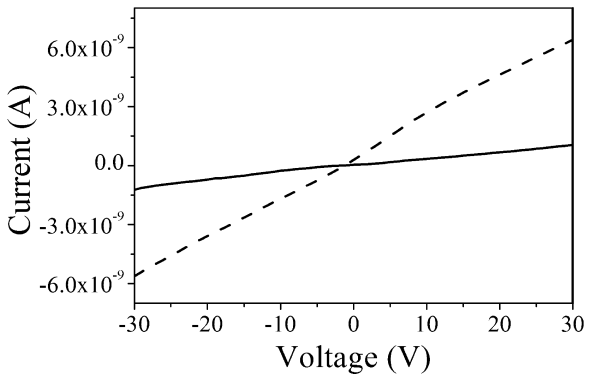

Fig. 9. *I–V* curves of 15C5PDI LB films formed on water surface (solid line) and 0.005 mol L^{-1} potassium chloride surface (dash line).

of 15C5PDI deposited from the surface of ion-containing subphase had a long-range order across its thickness [22]. Compared with the LB films deposited from water, a small increase of average d-spacing (2.48 nm) was obtained, which results in a little bit larger orientation angle (72.5°) between PDI plane and substrate surface, revealing the slipped cofacial arrangement with an "edge-on" conformation of the 15C5PDI molecules in the LB films (Supplementary material, Scheme S3). In present case, the coordination of the K^+ ions with the crown ethers from the neighboring molecules increases the hydrophilicity and makes the plane of PDI more perpendicular to the surface of water, and closer packing is possible for the PDI rings and thus increases the distance between the interlayer [52]. This is in accordance with the results from π to *A* isotherms. In addition, a high-order diffraction in 15C5PDI LB films deposited from the surface of ion-containing subphase was found at 0.31 nm corresponding to the π-stacking, which is consistent with the typical distance for effective π–π stacking between aromatic molecules. Such effective co-facial π–π stacking among PDI rings of 15C5PDI molecules should be expected to decrease the barrier to charge transport, which in turn contributes to the higher conductivity revealed for the devices fabricated with the films (vide infra).

The morphology of the films formed on the surface of either water or ion-containing subphase was examined by atomic force microscope (AFM). The film prepared from the surface of water result in a membrane-like structure, which consisted of numerous nanoparticles with the average diameter of ca.50 nm, Fig. 8A. On the other hand, depending on the coordination bonding between 15-crown-5-ether groups and K^+ ions in cooperation with intermolecular π–π interaction between neighboring 15C5PDI molecules, the long one-dimensional (1D) nanofibrils with average width of ca. 75 nm, over 2 μm in length were obtained on the surface of the film formed on ion-containing subphase, Fig. 8B. The success in preparing 1D nanofibrils from 15C5PDI by introduce of potassium ions (KCl) was confirmed unambiguously by the elemental signatures of C, O, N and K in energy-dispersive spectrometry (EDS) as shown in the inset of Fig. 8B. The obvious difference on the morphology of the two kinds of 15C5PDI films indicates the effect of a synergistic interplay among noncovalent interactions, including π–π interaction, van der Waals, hydrophilic/hydrophobic, and metal–ligand coordination, on fine controlling and tuning the molecular packing conformation of PDI molecules in the corresponding films. It is worth note that the size- and morphology-adjustable nanostructures are highly desired for fabricating nano-scale molecular (opto)-electronic devices which often require a wide variety of channel lengths to achieve the optimum gate or optical modulation.

The uniform LB films of 15C5PDI with well-defined nanostructures would be promising candidates for applications in electronic devices. To demonstrate the potentials of these nanostructures, two kinds of 15C5PDI LB films (20 layers) formed on the surface of water (film **1**) and ion-containing subphase (film **2**) were carefully deposited onto glass substrates with ITO IDEs, respectively, and the electron conductivity measurement was conducted in situ. Fig. 9

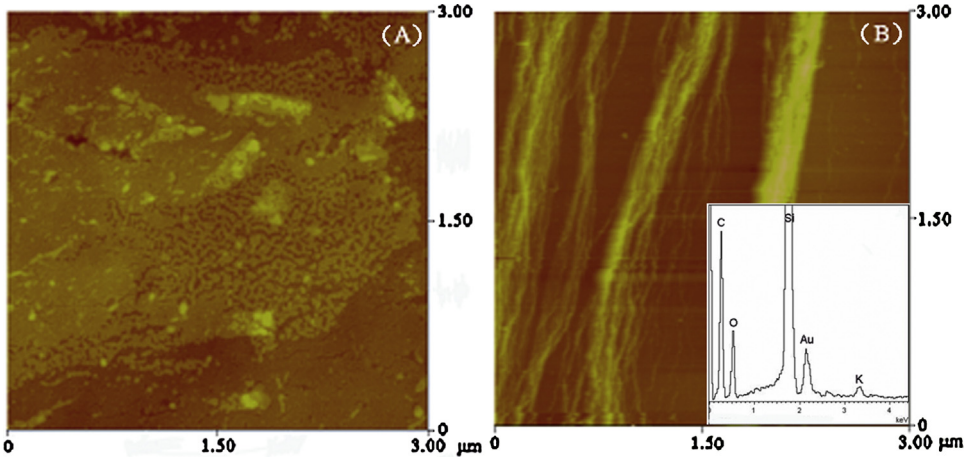

Fig. 8. AFM images of 15C5PDI LB film formed on water surface (A) and 0.005 mol L^{-1} potassium chloride surface (B).

shows the current–voltage (*I–V*) properties of film **1** and **2**. According to the equation reported in the literatures [35,36], the electronic conductivity is calculated to be about $(4.2 \pm 0.1) \times 10^{-9}$ S cm^{-1} for film **1** and $(6.3 \pm 0.4) \times 10^{-8}$ S cm^{-1} for film **2**, respectively. All experiments have been conducted at least three times on five different pieces of films to ensure reproducibility. The stable and reproduced *I–V* curves of different LB films of 15C5PDI are obtained and shown in Fig. S4. Comparing with film **1** formed on the pure water surface, the significantly improved conductive capability of the film **2** formed on the surface of ion-containing subphase, should be attributed to readily π-stacks with adjacent molecules and the better film crystallinity and higher ordered molecular arrangement in the film **2** of 15C5PDI molecules. The absence of traps and/or defects in the 1D nanofibrils with more efficient π–π stacks and metal–ligand coordination interactions should favor charge transport. It should be noted that no valuable *I–V* curve from the cast film of 15C5PDI molecules (the chloroform solution of 15C5PDI was cast onto glass substrates with ITO IDEs) was obtained due to its disordered. These aggregates with high current modulation could be useful for a wide range of electronic and sensor devices.

It is worth noting that, as shown in Fig. 6B, the fluorescence of LB films deposited from both water (line a) and aqueous KCl surface (line b) exhibited a significant quenching in the both case due to the formation of *H* aggregates. As a result, both the fluorescence quantum yield and lifetime of the resulting LB films could not be detected. It is difficult for us to scale non-emission properties with conductivity. However, the *I–V* measurements revealed that the conductivity of the LB films prepared on the surface of K^+ solution subphase is more than ca. 1 order of magnitude higher than those from water due to readily π-stacks with adjacent molecules and the better film crystallinity and higher ordered molecular arrangement in the film **2** of 15C5PDI molecules. Therefore, the conductivity of the films is more sensitive to film crystallinity and ordering than emission properties when the films have not emission properties detected.

4. Conclusion

In summary, we have synthesized successfully an unsymmetrical, 15-crown-5 functionalized perylene diimide, 15C5PDI. The fluorescent *J*-type and non-fluorescent *H*-type aggregates of 15C5PDI were obtained by K^+ ion-induced self-assembly in $CHCl_3$ solution and at the air/water interface, respectively. Aggregates with distinct morphologies and nanostructures for 15C5PDI were controllably prepared on the surface of water and K^+ ion-containing subphase. The *I–V* measurements revealed that the conductivity of the LB films prepared on the surface of K^+ solution subphase is more than ca. 1 order of magnitude higher than those from water. The present study would be valuable for the design and preparation of PDI-based nano-electronic and nano-optoelectronic devices with good performance.

Acknowledgments

Financial support from the Natural Science Foundation of China (21371073), Natural Science Foundation of Shandong Province (ZR2011BZ005) and University of Jinan in China is gratefully acknowledged.

Appendix A. Supplementary data

Supplementary data associated with this article can be found, in the online version, at http://dx.doi.org/10.1016/j.colsurfa.2014.10.021.

References

[1] X. Yang, X. Xu, H.F. Ji, Solvent effect on the self-assembled structure of an amphiphilic perylene diimide derivative, J. Phys. Chem. B 112 (2008) 7196–7202.
[2] Y. Chen, W. Su, M. Bai, J. Jiang, X. Li, Y. Liu, L. Wang, S. Wang, High performance organic field-effect transistors based on amphiphilic tris (phthalocyaninato) rare earth triple-decker complexes, J. Am. Chem. Soc. 127 (2005) 15700–15701.
[3] G. Lu, Y. Chen, Y. Zhang, M. Bao, Y. Bian, X. Li, J. Jiang, Morphology controlled self-assembled nanostructures of sandwich mixed (phthalocyaninato) (porphyrinato) europium triple-deckers. Effect of hydrogen bonding on tuning the intermolecular interaction, J. Am. Chem. Soc. 130 (2008) 11623–11630.
[4] D. Ke, C. Zhan, S. Xu, X. Ding, A. Peng, J. Sun, S. He, A.D.Q. Li, J. Yao, Self-assembled hollow nanospheres strongly enhance photoluminescence, J. Am. Chem. Soc. 133 (2011) 11022–11025.
[5] S. Ghosh, X. Li, V. Stepanenko, F. Würthner, Control of *H*- and *J*-type (stacking by peripheral alkyl chains and self-sorting phenomena in perylene bisimide homo- and heteroaggregates, Chem. Eur. J. 14 (2008) 11343–11357.
[6] L. Zang, Y. Che, J.S. Moore, One-dimensional self-assembly of planar π-conjugated molecules: adaptable building blocks for organic nanodevices, Acc. Chem. Res. 41 (2008) 1596–1608.
[7] Y. Chen, L. Wan, X. Yu, W. Li, Y. Bian, J. Jiang, Rational design and synthesis for versatile fret ratiometric sensor for Hg^{2+} and Fe^{2+}: a flexible 8-hydroxyquinoline benzoate linked bodipy-porphyrin dyad, Org. Lett. 21 (2011) 5774–5777.
[8] A. Hagfeldt, G. Boschloo, L. Sun, L. Kloo, H. Pettersson, Dye-sensitized solar cells, Chem. Rev. 110 (2010) 6595–6663.
[9] Y. Wang, Y. Chen, R. Li, S. Wang, W. Su, P. Ma, M.R. Wasielewski, X. Li, J. Jiang, Amphiphilic perylenetretracarboxyl diimide dimer and its application in field effect transistor, Langmuir 23 (2007) 5836–5842.
[10] A.L. Briseno, S.C.B. Mannsfeld, C. Reese, J.M. Hancock, Y. Xiong, S.A. Jenekhe, Z. Bao, Y. Xia, Perylenediimide nanowires and their use in fabricating field-effect transistors and complementary inverters, Nano Lett. 7 (2007) 2847–2853.
[11] B.A. Jones, M.J. Ahrens, M.-H. Yoon, A. Facchetti, T.J. Marks, M.R. Wasielewski, High-mobility air-stable n-type semiconductors with processing versatility: dicyanoperylene-3,4:9,10-bis(dicarboximides), Angew. Chem. Int. Ed. 43 (2004) 6363–6366.
[12] M. Bendikov, F. Wudl, D.F. Perepichka, Tetrathiafulvalenes, oligoacenenes, and their buckminsterfullerene derivatives: the brick and mortar of organic electronics, Chem. Rev. 104 (2004) 4891–4946.
[13] G.R. Hutchison, M.A. Ratner, T.J. Marks, Intermolecular charge transfer between heterocyclic oligomers. Effects of heteroatom and molecular packing on hopping transport in organic semiconductors, J. Am. Chem. Soc. 127 (2005) 16866–16881.
[14] M. Halik, H. Klauk, U. Zschieschang, G. Schmid, S. Ponomarenko, S. Kirchmeyer, W. Weber, Relationship between molecular structure and electrical performance of oligothiophene organic thin film transistors, Adv. Mater. 15 (2003) 917–922.
[15] A. Facchetti, M.H. Yoon, C.L. Stern, H.E. Katz, T.J. Marks, Building blocks for n-type organic electronics: regiochemically modulated inversion of majority carrier sign in perfluoroarene-modified polythiophene semiconductors, Angew. Chem. Int. Ed. 42 (2003) 3900–3903.
[16] Q. Miao, M. Lefenfeld, T.Q. Nguyen, T. Siegrist, C. Kloc, C. Nuckolls, Self-assembly and electronics of dipolar linear acenes, Adv. Mater. 17 (2005) 407–412.
[17] J.E. Anthony, D.L. Eaton, S.R. Parkin, A road map to stable, soluble, easily crystallized pentacene derivatives, Org. Lett. 4 (2002) 15–18.
[18] J.E. Anthony, J.S. Brooks, D.L. Eaton, S.R. Parkin, Functionalized pentacene: improved electronic properties from control of solid-state order, J. Am. Chem. Soc. 123 (2001) 9482–9483.
[19] H. Meng, M. Bendikov, G. Mitchell, R. Holgeson, F. Wudl, Z. Bao, T. Siegrist, C. Kloc, C.H. Chen, Tetramethylpentacene remarkable absence of steric effect on field effect mobility, Adv. Mater. 15 (2003) 1090–1093.
[20] G. Giri, E. Verploegen, S.C.B. Mannsfeld, S.A. Evrenk, D.H. Kim, S.Y. Lee, H.A. Becerril, A.A. Guzik, M.F. Toney, Z. Bao, Tuning charge transport in solution-sheared organic semiconductors using lattice strain, Nature 480 (2011) 504–508.
[21] J. Feng, Y. Zhang, C. Zhao, R. Li, W. Xu, X. Li, J. Jiang, Cyclophanes of perylene tetracarboxylic diimide with different substituents at bay positions, Chem. Eur. J. 14 (2008) 7000–7010.
[22] N. An, Y. Shi, J. Feng, D. Li, J. Gao, Y. Chen, X. Li, N-channel organic thin-film transistors based on a soluble cyclized perylene tetracarboxylic diimide dimer, Org. Electron. 14 (2013) 1197–1203.
[23] K. Balakrishnan, A. Datar, T. Naddo, J. Huang, R. Oitker, M. Yen, J. Zhao, L. Zang, Effect of side-chain substituents on self-assembly of perylene diimide molecules: morphology control, J. Am. Chem. Soc. 128 (2006) 7390–7398.
[24] W. Su, Y. Zhang, C. Zhao, X. Li, J. Jiang, Self-assembled organic nanostructures: effect of substituents on the morphology, ChemPhysChem 8 (2007) 1857–1862.
[25] L.E. Sinks, B. Rybtchinski, M. Iimura, B.A. Jones, A.J. Goshe, X. Zuo, D.M. Tiede, X. Li, M. Wasielewski, Self-assembly of photofunctional cylindrical nanostructures based on perylene-3,4:9,10-bis (dicarboximide), Chem. Mater. 17 (2005) 6295–6303.
[26] A. Gesquiere, P. Jonkheijm, F.J.M. Hoeben, A.P.H.J. Schenning, S. De Feyter, F.C. De Schryver, E.W. Meijer, 2D-Structures of quadruple hydrogen bonded oligo(p-phenylenevinylene)s on graphite: self-assembly behavior and expression of chirality, Nano. Lett. 4 (2004) 1175–1179.

[27] A.P.H. Schenning, J.V. Herrikhuyzen, P. Jonkheijm, Z. Chen, F. Würthner, E.W. Meijer, Photoinduced electron transfer in hydrogen-bonded oligo (p-phenylene vinylene)-perylene bisimide chiral assemblies, J. Am. Chem. Soc. 124 (2002) 10252–10253.
[28] Y. Chen, Y. Feng, J. Gao, M. Bouvet, Self-assembled aggregates of amphiphilic perylene diimide-based semiconductor molecules: effect of morphology on conductivity, J. Colloid Interface Sci. 368 (2012) 387–394.
[29] L. Xue, Y. Wang, Y. Chen, X. Li, Aggregation of wedge-shaped perylenetetracarboxylic diimides with a different number of hydrophobic long alkyl chains, J. Colloid Interface Sci. 350 (2010) 523–529.
[30] H. Wu, L. Xue, Y. Shi, Y. Chen, X. Li, Organogels based on J-and H-type aggregates of amphiphilic perylenetetracarboxylic diimides, Langmuir 27 (2011) 3074–3082.
[31] L. Xue, H. Wu, Y. Shi, H. Liu, Y. Chen, X. Li, Supramolecular organogels based on perylenetetracarboxylic diimide dimer or hexamer, Soft Matter 7 (2011) 6213–6221.
[32] A. You, J. Gao, D. Li, M. Bouvet, Y. Chen, Effects of metal–ligand coordination on the self-assembly behaviour of a crown ether functionalised perylenetetracarboxylic diimide, Supramol. Chem. 24 (2012) 851–858.
[33] M.C. Petty, Langmuir–Blodgett Films: An Introduction, Cambridge University Press, Cambridge, 1996.
[34] Y. Chen, Y. Kong, Y. Wang, P. Ma, M. Bao, X. Li, Supramolecular self-assembly study of a flexible perylenetetracarboxylic diimide dimer in Langmuir and Langmuir–Blodgett films, J. Colloid Interface Sci. 330 (2009) 421–427.
[35] Y. Chen, M. Bouvet, T. Sizun, Y. Gao, C. Plassard, E. Lesniewsk, J. Jiang, Facile approaches to build ordered amphiphilic tris(phthalocyaninato) europium triple-decker complex thin films and their comparative performances in ozone sensing, Phys. Chem. Chem. Phys. 12 (2010) 12851–12861.
[36] H. Ahn, A. Chandekar, B. Kang, C. Sung, J.E. Whitten, Electrical conductivity and vapor-sensing properties of ω-(3-thienyl)alkanethiol-protected gold nanoparticle films, Chem. Mater. 16 (2004) 3274–3278.
[37] S.K. Lee, Y. Zu, A. Herrmann, Y. Geerts, K. Müllen, A.J. Bard, Electrochemistry, spectroscopy and electrogenerated chemiluminescence of perylene, terrylene, and quaterrylene diimides in aprotic solution, J. Am. Chem. Soc. 121 (1999) 3513–3520.
[38] M. Kasha, H.R. Rawls, M.A. El-Bayoumi, The excition model in molecular spectroscopy, Pure Appl. Chem. 11 (1965) 371–392.
[39] F. Würthner, C. Thalacker, S. Diele, C. Tschierske, Fluorescent J-type aggregates and thermotropic columnar mesophases of perylene bisimide dyes, Chem. Eur. J. 7 (2001) 2245–2253.
[40] M.R. Wasielewski, Self-assembly strategies for integrating light harvesting and charge separation in artificial photosynthetic systems, Acc. Chem. Res. 42 (2009) 1910–1921.
[41] Z. Chen, U. Baumeister, C. Tschierske, F. Würthner, Effect of core twisting on self-assembly and optical properties of perylene bisimide dyes in solution and columnar liquid crystalline phases, Chem. Eur. J. 13 (2007) 450–465.
[42] Y. Ma, C. Wang, Y. Zhao, Y. Yu, C. Han, X. Qiu, Z. Shi, Perylene diimide dyes aggregates: optical properties and packing behavior in solution and solid state, Supramol. Chem. 19 (2007) 141–149.
[43] E.H. Beckers, Z. Chen, S.C.J. Meskers, P. Jonkheijm, A.P.H.J. Schenning, X.Q. Li, P. Osswald, F. Wurthner, R.A.J. Janssen, The importance of nanoscopic ordering on the kinetics of photoinduced charge transfer in aggregated π-conjugated hydrogen-bonded donor–acceptor systems, J. Phys. Chem. B 110 (2006) 16967–16978.
[44] N. Sheng, R. Li, C.F. Choi, W. Su, D.K.P. Ng, X. Cui, K. Yoshida, N. Kobayashi, J. Jiang, Heteroleptic bis(phthalocyaninato) europium(iii) complexes fused with different numbers of 15-crown-5 moieties. Synthesis, spectroscopy, electrochemistry, and supramolecular structure, Inorg. Chem. 45 (2006) 3794–3802.
[45] J. Song, Q. Tian, J. Gao, H. Wu, Y. Chen, X. Li, Controlled preparation of Cds nanoparticle arrays in amphiphilic perylene tetracarboxylic diimides: organization, electron-transfer and semiconducting properties, CrystEngComm 16 (2014) 1277–1286.
[46] W. Xu, H. Chen, Y. Wang, C. Zhao, X. Li, S. Wang, Y. Weng, Photoinduced electron and energy transfer in dyads of porphyrin dimer and perylene tetracarboxylic diimide, ChemPhysChem 9 (2008) 1409–1415.
[47] T. Van der Boom, R.T. Hayes, Y. Zhao, P.J. Bushard, E.A. Weiss, M.R. Wasielewski, Charge transport in photofunctional nanoparticles self-assembled from zinc 5,10,15,20-tetrakis(perylenediimide)porphyrin building blocks, J. Am. Chem. Soc. 124 (2002) 9582–9590.
[48] F. Würthner, Perylene bisimide dyes as versatile building blocks for functional supramolecular architectures, Chem. Commun. 14 (2004) 1564–1579.
[49] W. West, S. Pearce, The dimeric state of cyanine dyes, J. Phys. Chem. 69 (1965) 1894–1903.
[50] J. Kim, D.T. McQuade, S.K. McHugh, T.M. Swager, Ion-specific aggregation in conjugated polymers: highly sensitive and selective fluorescent ion chemosensors, Angew. Chem. Int. Ed. 39 (2000) 3868–3872.
[51] F. Würthner, Z. Chen, V. Dehm, V. Stepanenko, One-dimensional luminescent nanoaggregates of perylene bisimides, Chem. Commun. 11 (2006) 1188–1190.
[52] Y. Chen, S. Zhao, X. Li, J. Jiang, Tuning the arrangement of mono-crown ether-substituted phthalocyanines in Langmuir–Blodgett films by the length of alkyl chains and the cation in subphase, J. Colloid Interface Sci. 289 (2005) 200–205.